

# Point-contact spectroscopy in $MgB_2$ single crystals in magnetic field

D. Daghero<sup>a</sup>, R. S. Gonell<sup>a</sup>, G. A. Ummarino<sup>a</sup>, V. A. Stepanov<sup>b</sup>, J. Jun<sup>c</sup>, S. M. Kazakov<sup>c</sup>, and J. Karpinski<sup>f</sup>

<sup>a</sup>INFM - Dipartimento di Fisica, Politecnico di Torino, Corso Duca degli Abruzzi 24, 10129 Torino, Italy

<sup>b</sup>P. N. Lebedev Physical Institute, Russian Academy of Sciences, Leninskiy Pr. 53, 119991 Moscow, Russia

<sup>c</sup>Solid State Physics Laboratory, ETH, CH-8093 Zurich, Switzerland

We present the results of a spectroscopic study of state-of-the-art  $MgB_2$  single crystals, carried out by using a modified point-contact technique. The use of single crystals allowed us to obtain point contacts with current injection either parallel or perpendicular to the ab planes. The effect of magnetic fields up to 9 T on the conductance spectra of these contacts is here thoroughly studied, for both  $B$  parallel and perpendicular to the ab planes. The complete temperature evolution of the upper critical field of the  $\sigma$  band is determined for the first time, and quantitative information about the upper critical field of the  $\sigma$  band and its anisotropy is obtained. Finally, by exploiting the different effect of a magnetic field applied parallel to the ab planes on the two band systems, the partial contributions of the  $\sigma$  and  $\pi$  bands to the total conductance are obtained separately. Fitting each of them with the standard BTK model yields a great reduction of the uncertainty on  $H_{c2}^{\sigma}$  and  $H_{c2}^{\pi}$ , whose complete temperature dependence is obtained with the greatest accuracy.

## 1. Introduction

About two years after the discovery of superconductivity in  $MgB_2$ , the validity of the two-gap model [1,4] in describing the superconducting and normal-state properties of this material has been confirmed by a large number of experimental evidences. Within this model, the complex electronic band structure of  $MgB_2$  [5,8] is approximated by one quasi-2D band and one 3D band, featuring two gaps of very different amplitude,  $\Delta_{\sigma}$  and  $\Delta_{\pi}$ . The different spatial character of the two bands arises from the layered structure of the material, that is also expected to give rise to macroscopic anisotropy in some relevant physical quantities, e.g. penetration depth, coherence length, and upper critical fields. The value of the anisotropy ratio  $\gamma = H_{c2}^{\sigma}/H_{c2}^{\pi}$  in  $MgB_2$  has long been a matter of debate, because of the large spread of values measured in films and polycrystalline samples [9]. To this regard, the recent setup of efficient crystal-growth techniques has thus been an essential improvement. As a matter of

fact, torque magnetometry [10] and thermal conductivity measurements [11] in high-quality single crystals have given substantially consistent values of the upper critical fields as a function of the temperature.

In this paper, we present the results of directional point-contact spectroscopy (PCS) in state-of-the-art single crystals, in the presence of a magnetic field applied either parallel or perpendicular to the ab planes. The use of PCS, and the possibility of controlling the directions of both the injected current and the field, allowed us to study the effect of the magnetic field on each band system, separately. It turns out that the magnetic field strongly affects the superconductivity in the  $\sigma$ -band, irrespective of its orientation. An analysis of the conductance curves measured at different temperatures and various field intensities gives the temperature evolution of the  $\sigma$ -band upper critical field,  $H_{c2}^{\sigma} = \gamma H_{c2}^{\pi}$ , determined here for the first time. In contrast, the effect of the field on the  $\pi$  band is highly anisotropic. Our measurements indicate that the upper critical field of the  $\pi$  band for  $B$  parallel to the  $c$

---

Corresponding author. e-mail: ddaghero@polito.it

axis,  $B_{c2kC}$ , is higher than that measured by other groups on similar samples [10,11], possibly because of surface effects. Finally, the temperature dependence of the two gaps is obtained with unprecedented accuracy, by separating the partial  $\gamma$ - and  $\beta$ -band contributions to the total conductance by means of a suitable magnetic field.

## 2. Experimental set up

All the details about the sample preparation are given in the paper by Karpinski et al. in this same issue. The  $MgB_2$  single crystals we used for our measurements were about  $0.6 \times 0.6 \times 0.04 \text{ mm}^3$  in size, even though the growth technique allows obtaining even larger samples. The crystals were etched with 1% HCl in dry ethanol, to remove possible deteriorated surface layers. The critical temperature of the crystals, measured by AC susceptibility, is  $T_c = 38.2 \text{ K}$  with  $T_c \approx 0.2 \text{ K}$ .

Possibly because of the extreme hardness of the crystals, point contacts obtained by pressing a metallic tip against the crystal surface were found to fail the essential requirements of reproducibility and mechanical stability upon thermal cycling. Therefore, we made the contacts by using as a counterelectrode either a small drop of silver conductive paint ( $\approx 50 \text{ nm}$ ) or a small spot of indium. The control of the junction characteristics (which, in the conventional technique, is obtained by moving the tip) was a little more difficult in this case. However, by applying short voltage pulses we were able to change the characteristics of the contact, until satisfactory stability and reproducibility were attained.

Of course, the apparent size of our contacts is much greater than that required to have ballistic transport across the junction [12]. Actually, the effective electrical contact occurs via parallel micro-bridges in the spot area, that can be thought of as Sharvin contacts. This assumption is supported a posteriori by the absence of heating effects in the conductance curves of all our junctions. Moreover, by using in the Sharvin formula the experimental resistance of our contacts (that always fell in the range  $10 - 50 \text{ m}\Omega$ ) the estimated mean free path  $\ell = 600 \text{ \AA}$ , and the residual resistivity  $\rho_0 \approx 2 \text{ m}\Omega$  [1] one obtains that, at

least in the higher-resistance junctions, the transport is ballistic even if a single contact is established.

The contacts were positioned on the crystal surfaces so as to inject the current along the  $c$  axis or along the  $ab$  planes. In the following, we will refer to them as " $c$ -axis contacts" and " $ab$ -plane contacts". Notice that, when the potential barrier at the interface is small as in our case, the current is injected in a cone whose angle is not negligible, and becomes equal to  $\pi/2$  in the ideal case of no barrier. Anyway, the probability for electrons to be injected along an angle  $\theta$  in the cone is proportional to  $\cos \theta$  [13] so that the (main) direction of current injection can still be defined.

## 3. Experimental results and discussion

### 3.1. Magnetic field parallel to the $c$ axis

Figure 1 shows the normalized conductance curves of an  $ab$ -plane contact, for increasing intensities of the magnetic field applied parallel to the  $c$  axis. The differential conductance  $dI/dV$  was numerically calculated from the measured  $I - V$  characteristic of the junction. The normalization was made by dividing the experimental  $dI/dV$  vs.  $V$  curves by the linear or quartic function that best fits them for  $|V| \geq 30 \text{ mV}$ . The zero-field curve shows two peaks at  $V \approx \pm 2.7 \text{ mV}$  and  $V \approx \pm 7.2 \text{ mV}$ , clearly related to the two gaps  $\gamma$  and  $\beta$ , respectively. On increasing the magnetic field intensity, the peaks related to the smaller gap,  $\gamma$ , are quickly suppressed, and they finally disappear at  $B = 0.9 \text{ T}$ . On the contrary, the features connected to the large gap,  $\beta$ , look practically unchanged. The whole shape of the conductance curves changes very little if the field slightly exceeds the value  $B = 1 \text{ T}$ , suggesting that in this magnetic-field region the  $\beta$ -band is quite robust. On further increasing the field intensity, the two peaks corresponding to  $\beta$  decrease in amplitude and gradually shift to lower energies, i.e. the large gap gradually closes. At  $B = 4 \text{ T}$ , however, the normalized conductance is still far from being flat. This means that, at the liquid helium temperature, the upper critical field of the  $\beta$ -band for  $B \parallel c$  is greater than 4 Tesla, in

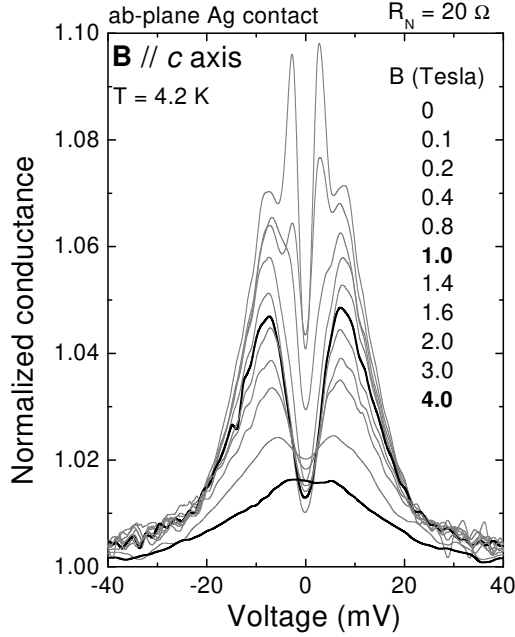


Figure 1. Effect of a magnetic field of increasing intensity, applied parallel to the  $c$  axis, on the conductance curves of a Ag/MgB<sub>2</sub> point contact with current injection mainly along the  $ab$  plane. All the curves were measured at  $T = 4.2$  K. Thick black lines represent the experimental curves at  $B = 1$  T and  $B = 4$  T.

contrast to the value  $H_{c2}^{kc} = 30$  kOe given by recent torque magnetometry [10] and thermal conductivity measurements [11]. The possible reason for this discrepancy will be discussed later on.

Let us discuss for a while the quick suppression of the small-gap features and their disappearance at  $B = 1$  T. This result was already obtained by point-contact measurements in polycrystalline samples [14], and was interpreted as due to the selective suppression of the superconductivity in the bands. In our case, the use of single crystals allows giving more convincing arguments to support this interpretation, i.e. to show that the magnetic field of 1 Tesla really destroys the superconductivity in the bands, without affecting the bands.

As a matter of fact, in Figure 2 the zero-field

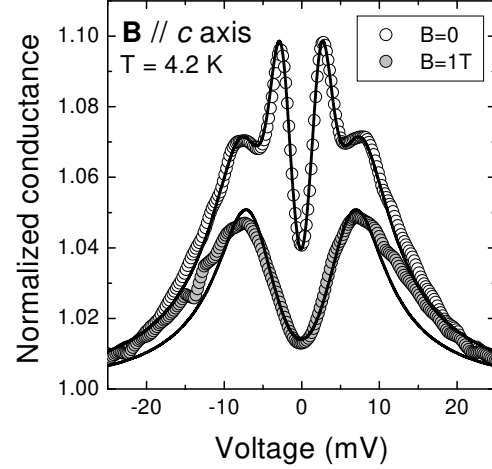


Figure 2. The experimental normalized conductance curves at  $B = 0$  (open symbols) and  $B = 1$  T (filled symbols) already reported in Fig. 1 compared to the theoretical curves. The solid line superimposed to the upper curve is a best-fitting BTK function (see eq.1). The solid line superimposed to the lower curve is not a best-fitting curve, but the function obtained from the previous one by taking  $\eta = 1$  (see eq.2). For details see the text.

curve (open symbols) and the curve in a field of 1 T (filled symbols) are compared. The solid line superimposed to the former is its best-fitting curve obtained with the BTK model [15] generalised to the case of two bands, in which the normalized conductance is expressed by a weighed sum of the partial BTK conductances of the and bands:

$$G = w G_1 + (1 - w) G_2 : \quad (1)$$

In practice, the total conductance across the junction is thought of as the parallel of two (independent) channels. Here  $w$  is the weight of the channel connected to the band, i.e. the partial contribution of the band to the total conductance.  $w$  is a function of the plasma frequencies  $\omega_p$  and  $\omega_p'$ , that are much different in the  $ab$ -plane and along the  $c$  axis. As a result,  $w$  depends on the angle  $\theta$  between the direction of current injection and the boron planes [3]. For current injection purely along the  $ab$  plane, the value  $w = 0.66$  is

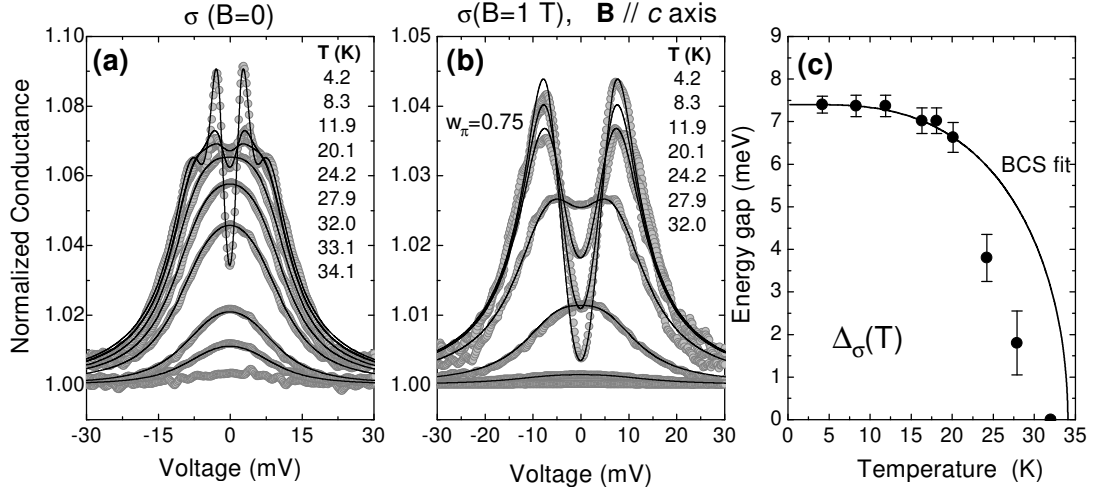


Figure 3. (a) Temperature dependence of the experimental normalized conductance of a *ab*-plane Ag contact ( $R_N = 20$ ). Solid lines are the best-fitting functions given by eq.1. (b) Same as in (a) but with a magnetic field of 1 Tesla applied parallel to the *c* axis. Solid lines represent the best-fitting curves given by eq.2. (c) Thermal evolution of the large gap as obtained from the fit of the curves in (b).

theoretically predicted [3].

The fitting function expressed by eq.1 contains 7 adjustable parameters ( $\epsilon$  and  $\delta$ , the broadening parameters and  $Z_1$ , the barrier transparency coefficients  $Z_1$  and  $Z_2$ , plus the weight factor  $w$ ) so there is some uncertainty in the choice of the best-fitting values, especially as far as  $Z_1$  and  $Z_2$  are concerned. The curve superimposed to the zero-field conductance in Fig. 2 was obtained by using:  $\epsilon = 2.8$  meV,  $\delta = 7.2$  meV,  $Z_1 = 0.48$ ,  $Z_2 = 0.94$ ,  $\epsilon_1 = 1.49$  meV,  $\epsilon_2 = 3.3$  meV, and finally  $w = 0.75$ . The gap amplitudes agree very well with those predicted by the two-band model [3]. The disagreement between the predicted value of  $w$  (0.66) and that given by the fit (0.75) is simply due to the fact that, as previously pointed out, the current is injected within a solid angle rather than along a precise direction. As a matter of fact, it can be shown that the value  $w = 0.75$  is compatible with an injection cone about  $26^\circ$  wide [16].

If the superconductivity in the  $\sigma$  band is destroyed without affecting the  $\pi$  band, the total conductance across the junction is expressed by:

$$G = w + (1 - w) : \quad (2)$$

which is obtained by taking  $\epsilon = 1$  in eq.1, and

thus only contains the free parameters  $\epsilon$ ,  $\delta$ , and  $Z_1$ , plus the weight factor  $w$ . This is indeed the functional form of the curve shown in Fig. 2, superimposed to the conductance curve at  $B = 1$  Tesla. All the parameters are unchanged with respect to the zero-field curve, apart from the barrier parameter that was set to  $Z_1 = 0.56$  to adjust the height of the theoretical curve. It is clear that this function reproduces both the position of the conductance peaks and the shape of the conductance well around zero bias. This demonstrates that a field of 1 Tesla parallel to the *c* axis really destroys the superconductivity in the  $\sigma$  band, without affecting the amplitude of the  $\pi$ -band gap.

One can now wonder whether this is true also when the temperature is increased, or rather a temperature  $T < T_c$  exists at which also the bands start being affected by the field. Fig. 3 reports the temperature dependence of the experimental curves of the same *ab*-plane contact discussed so far, in zero field (a) and in the presence of a field of 1 Tesla parallel to the *c* axis (b). Even at a first sight, it is clear that the curves in zero field become almost flat at  $T = 34.1$  K, which is therefore close to the critical temperature of the junction, while the curves in the presence

of the  $\epsilon$  d { that only contain the  $\epsilon$ -band conductance { atten at  $T = 32$  K. This suggests by itself that the magnetic  $\epsilon$  d causes the transition to the normal state at a temperature lower than  $T_c$ . This conclusion can be further supported by extracting the temperature dependence of  $\epsilon$  from the conductance curves in Fig. 3b, which requires fitting the experimental curves. The solid lines superimposed to the experimental data in (a) and (b) represent the relevant best-fitting curves obtained by using eq.1 and eq.2, respectively. In both cases, the weight  $w$  was taken as temperature-independent. The barrier parameters  $Z_1$  and  $Z_2$  were kept (almost) constant at the increase of the temperature. Instead, the broadening parameters  $\epsilon_1$  and  $\epsilon_2$  given by the  $\epsilon$  increase with  $T$ . In the case of Fig. 3a,  $\epsilon_1$  varies between 1.49 and 2.29 meV, and  $\epsilon_2$  increases from 3.3 up to 3.6 meV;  $Z_1$  and  $Z_2$  vary from 0.94 to 0.8 and from 0.48 to 0.33, respectively. In the case of Fig. 3b, instead,  $\epsilon_1$  is equal to 3.7 meV at low  $T$  and increases rapidly on heating, while  $Z_1$  remain in the range between 0.6 and 0.45.

The thermal evolution of  $\epsilon$ , obtained by fitting the curves in Fig. 3b with the three-parameter function given by eq. 2, is reported in Fig. 3c (circles) together with a BCS-like curve (solid line). It is clear that the points sudden deviate from the BCS behaviour at  $T = 20$  K. Based on previous determinations of the temperature dependence of  $\epsilon$  in zero  $\epsilon$  d [16], we can rather safely assume that such a large deviation is due to the progressive closing of the large gap due to the magnetic  $\epsilon$  d. At  $T = 32$  K, the  $\epsilon$ -band gap disappears: this means that, at this temperature,  $B_{c2}^{kc} = 1$  T. A gain, this value is larger than that recently measured in the same crystals by other groups [10,11].

### 3.2. Magnetic $\epsilon$ d parallel to the ab planes

Fig. 4 shows the conductance curves of a  $\epsilon$ -plane in contact as a function of the intensity of the magnetic  $\epsilon$  d, applied parallel to the ab planes. Exactly as in Fig.1, the small-gap features are very easily disrupted by the  $\epsilon$  d. At  $B = 1$  T,  $\epsilon$  completely vanishes while  $\epsilon$  remains unchanged. Based on arguments similar

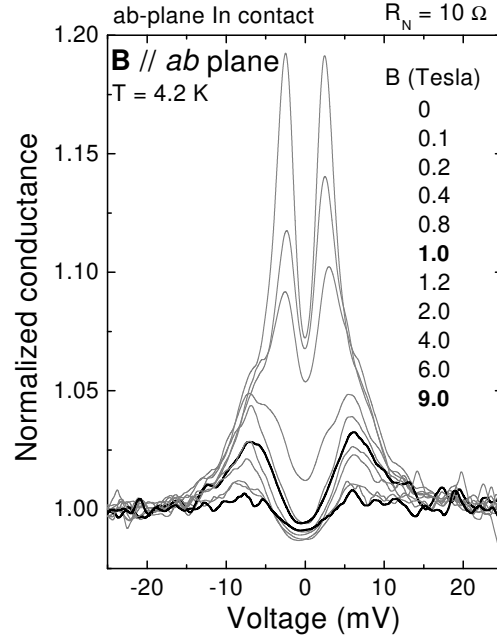


Figure 4. Magnetic-field dependence of the low-temperature normalized conductance curves of a  $\epsilon$ -plane in contact. The magnetic  $\epsilon$  d is applied parallel to the ab plane. Thick lines represent the curves at 1 T and 9 T.

to those used in the  $B \parallel c$  case, we can conclude that, at the liquid helium temperature, the upper critical  $\epsilon$  d of the  $\epsilon$  bands is isotropic, as shown in ref. [17], and takes the value  $B_{c2} = H_{c2} \approx 1$  T. Contrary to what happens in a magnetic  $\epsilon$  d applied parallel to the  $c$  axis, the conductance peaks associated to the  $\epsilon$ -band gap remain well distinguishable up to 9 T. A small decrease in the gap amplitude is observed above 4 T, together with an increase in the zero-bias conductance. It looks thus clear that, at 4.2 K, the critical  $\epsilon$  d of the band in the  $B \parallel ab$  case is much greater than 9 T, in agreement with other experimental findings.

As already done in the  $B \parallel c$  case, let us check whether the robustness of the  $\epsilon$  bands upon application of a  $\epsilon$  d of 1 Tesla persists at the increase of the temperature. Figure 5 reports the temperature evolution of the normalized conductance curves (symbols) in zero  $\epsilon$  d (a), and in the presence of a  $\epsilon$  d of 1 Tesla (b) parallel to

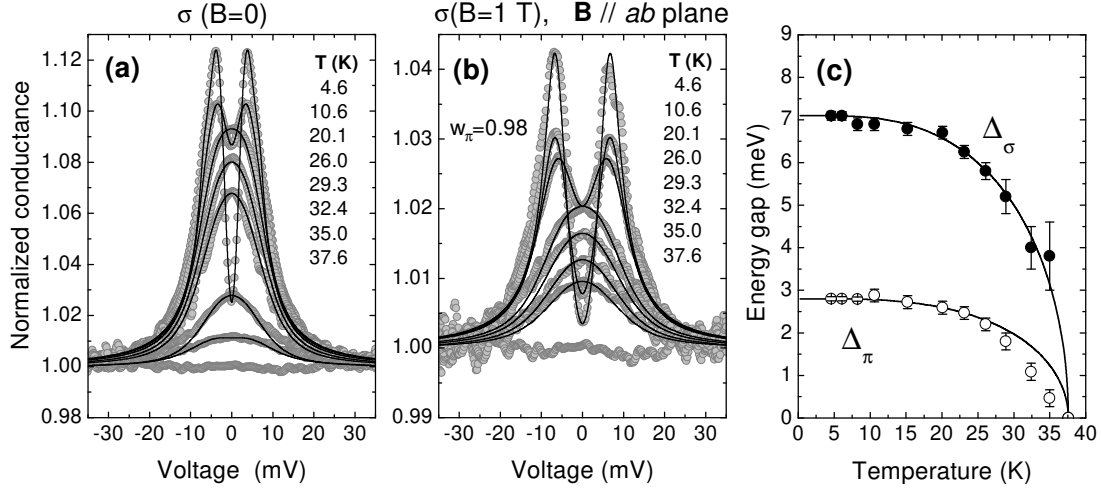


Figure 5. (a) Temperature dependence of the experimental normalized conductance of a c-axis In contact ( $R_N = 50 \Omega$ ). Solid lines are the best-fitting curves of the form given in eq.1. (b) Same as in (a) but in a magnetic field of 1 Tesla applied parallel to the ab plane. Lines: best-fitting curves expressed by eq.2. (c) Temperature dependence of the large gap  $\Delta_\sigma$  from the fit of the curves in (b), and of the small gap  $\Delta_\pi$  from the fit of the difference between the curves in (a) and (b) (see ref.[16] for details).

the ab plane. It is clearly seen that, in this case, all the curves become flat at the same temperature  $T = 37.6$  K (which is the critical temperature of the junction) indicating that the superconductivity in the  $\sigma$  band survives up to  $T_c$  even in the presence of the field. Solid lines in Figs. 5a and 5b represent the best-fitting curves obtained by using eqs.1 and 2, respectively. The value of the weight  $w_\pi = 0.98$  was determined by fitting the zero-field, low-temperature curve and then kept constant<sup>2</sup>. Let us disregard the values of the fitting parameters of the zero-field curves, as they are not essential for our reasoning. As far as the curves in Fig. 5b are concerned, the low-temperature values of the fitting parameters are:  $\Delta_\sigma = 7.1$  meV,  $\Delta_\pi = 1.75$  meV and  $Z = 0.58$ . At the increase of the temperature,  $\Delta_\sigma$  regularly increases up to 4.2 meV close to  $T_c$ , while  $Z$  slightly decreases down to 0.35. The temperature dependence of  $\Delta_\sigma$  obtained by the fit is reported in Fig. 5c (solid symbols) and compared to a BCS-like curve (solid line). In agreement

with previous experimental findings and theoretical predictions [2,3], the large gap is found to follow rather well the BCS curve. Incidentally, this confirms a posteriori that the  $\sigma$ -band gap is not affected by the field of 1 Tesla even at temperatures rather close to  $T_c$ . Also notice the much smaller error on the gap values with respect to measurements in polycrystalline samples, due to the reduction in the number of adjustable parameters (from 6 to 3) obtained by removing the band gap by means of the field [16].

An highly accurate determination of the temperature evolution of  $\Delta_\pi$  is possible as well, by subtracting from the total conductance the partial contribution of the  $\sigma$  band. In practice, each experimental curve in Fig. 5b is subtracted from the curve in zero field measured at the same temperature, as discussed elsewhere [16], and the resulting curve is fitted by a function of the form  $\Delta_\pi = w(\Delta_\sigma - 1)$ , with  $w = 0.98$ . The temperature dependence of  $\Delta_\pi$  obtained from the fit is shown in Fig. 5c (open symbols) and compared to a BCS-like behaviour (solid line). At  $T \approx 20$  K,  $\Delta_\pi$  deviates from the BCS curve of an amount which is well greater than our experimental un-

<sup>2</sup>For current injection purely along the ab planes the predicted value of the weight is  $w_\pi = 0.99$ . Our value is compatible with a current injection cone of about  $60^\circ$ .

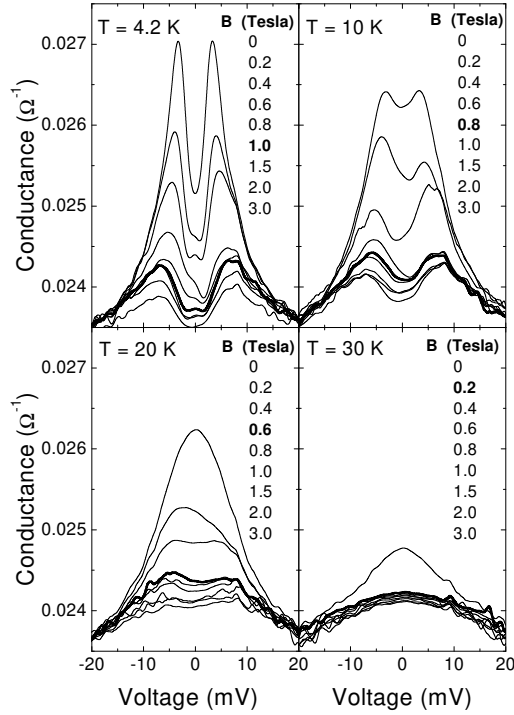


Figure 6. Unnormalized conductance curves of a  $c$ -axis In contact ( $R_N = 42 \Omega$ ) in a magnetic field of increasing intensity, applied parallel to the  $ab$  plane. Each panel refers to a different temperature, indicated in the graph.

certainty. This deviation is indeed predicted by the two-band model [2,3] but its unquestionable determination was impossible so far, because of the very large error affecting the gap values near  $T_c$ .

### 3.3. Temperature dependence of $B_{c2}$

Finally, let us determine the temperature evolution of the critical field of the  $\pi$  band, whose value at 4.2 K has been evaluated by analyzing the curves in Figs. 1 and 4. Fig. 6 reports the unnormalized (i.e., as measured) conductance curves of a  $c$ -axis contact, in the presence of a magnetic field applied parallel to the  $ab$  planes, at four temperatures: 4.2, 10, 20 and 30 K. Based on our previous finding that  $B_{c2kab} = B_{c2kc} = 1$  T at

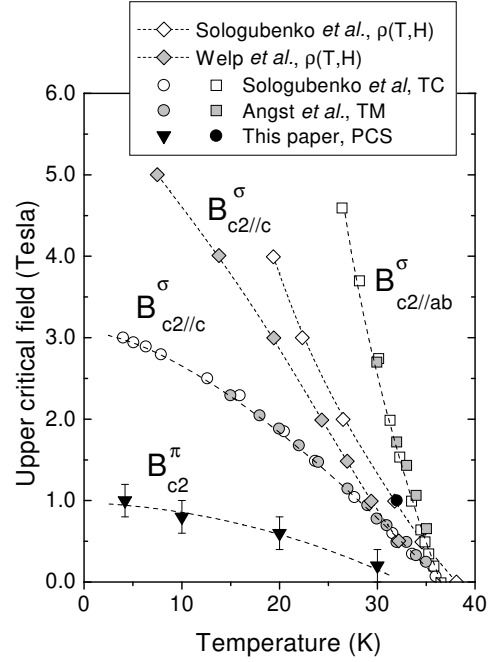


Figure 7. Phase diagram of  $MgB_2$  as it results from different kinds of measurements (TM = torque magnetometry, TC = thermal conductivity, PCS = point-contact spectroscopy, (T;H) = resistivity) carried out in single crystals. Lines are only guides to the eye.

4.2 K, and on the essentially isotropic character of the  $\pi$  bands [5,8,17] we will assume that the above equality holds at any temperature. The use of a  $c$ -axis contact emphasizes the  $\pi$ -band contribution to the conductance, but makes it more difficult to distinguish the (very small)  $\sigma$ -band features that survive after the removal of  $\pi$ . However, we expect that, just above  $B_{c2}$ , the conductance curves should be (relatively) field-independent, as long as the residual  $\pi$ -band gap is not suppressed. The curve that marks the beginning of this "saturation" is represented by a thick curve in the four panels of Fig. 6<sup>3</sup>. At 4.2, 10 and 20 K a residual gap-like feature is clearly observed in these curves, thus indicating the persistence of superconductivity in the  $\pi$  bands. At

<sup>3</sup>Notice that only the curves at some representative field intensities are reported for clarity.

$T = 30$  K the saturation occurs at  $B \approx 0.2$  T and above this field only minor changes in the conductance are observed. Since the upper critical field of  $MgB_2$  in the  $B \parallel ab$  case is, even at this temperature, at least one order of magnitude greater than 0.2 T [10,11,18], there is no doubt that this saturation is due to the removal of the  $\gamma$ -band gap alone.

The values of the magnetic field intensities that give rise to this saturation, and that we interpret as  $B_{c2}$ , are reported in Fig.7 (black triangles) together with the results of torque magnetometry [10], resistivity [11,18] and thermal conductivity measurements [11]. There are two points that are worth mentioning: the clear overestimation of  $B_{c2kc}$  by transport measurements, and the fact that all the critical fields determined by bulk measurements (e.g. thermal conductivity and torque magnetometry) vanish at a temperature  $T < T_c$ , where  $T_c$  is determined by the resistive transition. These puzzling results have been recently interpreted as due to the existence of an additional phase with enhanced critical parameters ( $T_c$  and  $H_{c2}$ ), probably related to surface effects that seem to be strongly suppressed by in-plane magnetic fields [18]. If this is the case, the results of surface-sensitive measurements might be sensibly different from those of bulk-sensitive techniques. This is an important point in discussing our results, since PCS is intrinsically a surface-sensitive probe. As a matter of fact, the value we determined for  $B_{c2kc}$  (black circle) is well compatible with the results of resistive measurements by Solgubenko et al., that were carried out on similar single crystals. Moreover, the observation of  $\gamma$ -band superconductivity at 4.2 K in a field of 4 T parallel to the  $c$  axis (see Fig.1) further supports this picture.

In conclusion, we have presented the results of a systematic study of  $MgB_2$  by means of point-contact spectroscopy in the presence of a magnetic field. The use of single crystals has allowed us to control the direction of both the current injection and the applied magnetic field. Consequently, we have been able to study the effect of the magnetic field on each band separately, and to determine for the first time the temperature dependence of the upper critical field of the isotropic

bands. As far as the  $\gamma$ -bands are concerned, the effect of the magnetic field has been confirmed to be strongly anisotropic. The obtained value of the upper critical field  $B_{c2kc}$  is higher than that measured on the same crystals by torque magnetometry and thermal conductivity, but agrees very well with the results of transport measurements. Finally, by exploiting the directionality of the point contacts and the different effect of the magnetic field on the two band systems, we have selectively destroyed the superconductivity in the  $\gamma$ -bands. This procedure allows separating the partial contributions of the  $\gamma$  and  $\sigma$  bands to the total conductance of the point contacts. Fitting each partial conductance with the standard BTK model, we have determined with great accuracy the temperature dependence of the two gaps, confirming the predictions of the two-gap models appeared in literature.

This work was supported by the INFM Project PRA-UMBRA and by the INTAS project "Charge transport in metal-diboride thin films and heterostructures".

## REFERENCES

1. H. Suhl, B.T. Matthias, and L.R. Walker, Phys. Rev. Lett. 3, 552 (1959).
2. A.Y. Liu, I.I. Mazin, and J. Kortus, Phys. Rev. Lett. 87, 87005 (2001).
3. A. Brinkman et al., Phys. Rev. B 65, 180517(R) (2001).
4. I.I. Mazin et al., cond-mat/0204013.
5. J. Kortus et al., Phys. Rev. Lett. 86, 4656 (2001).
6. S.V. Shulga et al., cond-mat/0103154.
7. J.M. An and W.E. Pickett, Phys. Rev. Lett. 86, 4366 (2001).
8. Y. Kong, O.V. Dolgov, O. Jepsen, and O.K. Andersen, Phys. Rev. B 64, 020501(R) (2001).
9. C. Buzea and T. Yamashita, Supercond. Sci. Technol. 14, R115 (2001).
10. M. Angst et al., Phys. Rev. Lett. 88, 167004 (2002).
11. A.V. Solgubenko et al., Phys. Rev. B 66, 014504 (2002).
12. A.M. Duif, A.G.M. Jansen, and P. Wyder, J. Phys.: Condens. Matter 1, 3157 (1989).
13. S. Kashiwaya and Y. Tanaka, Rep. Prog. Phys. 63, 1641 (2000).
14. P. Szabo et al., Phys. Rev. Lett. 87, 137005 (2001).
15. G.E. Blonder, M. Tinkham, and T.M. Klapwijk, Phys. Rev. B 25, 4515 (1982).
16. R.S. Gonelli et al., cond-mat/0208060.
17. F. Bouquet et al., cond-mat/0207141.
18. U. Welp et al., cond-mat/0203337.